



## Predicting the long-term durability of limestones subjected to freeze–thaw cycles (case study: Guilan province, north of Iran)

Maryam Dehban Avan Stakhri \* Mohammad Hossien Ghobadi , Hassan Mohseni

Department of Geology, Faculty of sciences, Bu-Ali Sina University, Hamedan, Iran

Received: 25 January 2021, Revised: 27 March 2021, Accepted: 18 April 2021

© University of Tehran

### Abstract

Mesozoic limestones with Cretaceous and Jurassic age are widely seen in the Guilan province, north of Iran. Regarding the climate of this area, the development of limestone with a high percent of  $\text{CaCO}_3$  (rather than 80%) and karst morphology development was investigated to evaluate the effect of freezing-thawing (F-T) cycles concerning the karst development. In this way, the physical and mechanical properties of the four lithology units (K11, K12, Km2, and Jkl) were assessed before and after F-T cycles to study the weathering effects. The survey of the petrography of rocks shows that the samples were grainstone and packstone type, according to Donham classification. The highest deterioration occurred in sample K12 after 60 F-T cycles. The physical and mechanical properties of rock samples such as  $\gamma$  (unit weight),  $w_a$  (water absorption),  $P_v$  (P-wave velocity), and UCS (uniaxial compressive strength) for both dry and saturated conditions, and after 60 cycles of freezing-thawing (F-T) were attained. The softening coefficient (K1) and freezing coefficient (K2) of samples were calculated using the UCS values. The F-T cycles caused significant losses in the UCS values. The measured  $V_p$  during the F-T cycles provided a suitable tool for calculating the damage value and decayed constant ( $\lambda$ ). This study showed that the F-T test is capable of creating microcrack and fractures within the rock as the initial factors for increasing the contact surface in the dissolution process. The increase in Dn (damage variable), porosity, water absorption, and decrease of  $V_p$  after 60 F-T cycles confirm this result. Also, the increase in tangent Young's modulus and decrease in strain show that the samples were brittle after 60 F-T periods. Therefore, it is concluded that the freezing and softening coefficient and  $V_p$  are effective tools for assessing the rock damage during F-T periods.

**Keywords:** Mesozoic Limestone, Freezing-thawing, Decay Value, Damage Variable, Wing Crack.

### Introduction

Some engineering properties of rocks such as bending strength, compression strength, deformability, and permeability are highly affected by freezing-thaw (F-T) cycles (Bellanger et al., 1993; Takarli et al., 2008; Beier & sego, 2009; Proskin et al., 2010; Saad et al., 2010; Jamshidi et al., 2015; Jamshidi et al., 2016). It has been theorized that water movement and relocation in micropores and its transformation to ice crystals create some stress due to capillary effect and hydraulic pressure (Powers & Helmuth, 1953; Everett, 1961; Setzer et al., 1997). The hydro–physico-mechanical parameters play the main role in the durability of Rock against frost. The intrinsic properties of rock such as total porosity, pore connectivity, pore size distribution, mechanical strength, mineralogy, grain-size, as well the environmental conditions have affected both the stone's durability and mechanism of frost weathering (Mutlutürk et al., 2004; Yavuz et al., 2006; Takarli et al., 2008; Tan et al., 2011; Bayram, 2012; Jamshidi et al., 2013). Given that during F-T cycles occurs temperature change with range -18 to +32°C, then

---

\* Corresponding author e-mail: mdehban@sci.basu.ac.ir

it is necessary to consider the anisotropic thermal behavior of calcite crystals. Calcite crystals show a positive dilation along the crystallographic c-axis in case of temperature increase, whereas that contracts along the a-axis (Andriani & Germinario 2014). These differential strains create especially internal stresses in tightly packed textures, which are shear, compression, and tensile in type. These stresses produce mainly at triple junctions and along grain boundaries (Shushakova et al. 2013; Andriani & Germinario 2014). The orientation, size, and morphology of crystals and grains have influenced by the intensity and distribution of stresses (Royer-Carfagni 1999; Siegesmund et al. 2000; Zeisig et al. 2002; Weiss et al. 2003; Koch & Siegesmund 2004; Plevova' et al. 2010; Andriani & Germinario 2014). Regarding the maximum principal stress and the elastic strain energy density are high in the pre-existing discontinuities, the role exerted by pre-existing discontinuities has to be considered as well. Where the material is more prone to thermal microcracking (Shushakova et al. 2011; Andriani & Germinario 2014); the more damaging can be observed for crystalline and sparitic carbonates due to this outcome (Siegesmund et al. 2010; Andriani & Germinario 2014). The stone remains more exposed and susceptible to attacks physical, chemical, and microbiological in type due to the increase of porosity through decementation and granular disintegration (Andriani & Walsh 2007; Luque et al. 2011; Andriani & Germinario 2014). The physical, mechanical, chemical and petrographical properties of limestone are fundamental to investigate karstification potential. Limestones existing in the northeast of Rudbar city (north of Iran) are exposed to at least 64 F-T cycles every year (Table 1). The 9% volumetric expansion of water compared to the original volume in the micropores during the freezing period is the primary reason for tensile stress concentration and damage of the micropores. The damage increases due to water flow through the fractured micropores when the rock is thawed. Rock damage in the regions with Mediterranean climatic depends on the number of F-T cycles in one year, temperature changes, rock type, applied stress, chemical weathering, moisture content, and porosity (Jamshidi et al., 2013). The effect of F-T cycles of various rocks is investigated using multiple laboratory tests. Most of these tests determine the impact of F-T on the mechanical and physical properties of stones such as uniaxial compression strength, tensile strength, P-wave velocity, compressibility, porosity, pore size distribution, permeability, and mineral content.

Engineering geological properties of carbonate rocks have been investigated by several researchers; e.g. Abdelhamid and et al., (2020), Gonzalez and et al., (2019), Hassanvand and et al., (2018), Yagiz, (2018), Eslami and et al., (2018), Hashemi and et al., (2018), Papay and Torok (2018), Jamshidi and et al., (2018), Fereidooni (2017), Walbert and et al., (2015), Walbert and et al., (2014), Bednarik and et al., (2014), Ghobadi and Torabi-Kaveh (2014), Ghobadi and Fereidooni (2013), Al-Omari (2013), Bayram (2012), Yagiz (2011), Gupta and Ahmed (2007), Yavuz and et al., (2006).

**Table1.** The 5 year's average of temperature, precipitation, and frosty days in the Deylaman station (2014-2019)

Month	Min-temperature(°C)	Max-temperature(°C)	Precipitation(mm)	Frosty days
April	-5.15	24.45	55.98	6
May	0.85	29.36	31.73	1
June	7.93	32.78	15.03	0
July	11	36.91	11.33	0
August	11.93	36.51	4.45	0
September	8.63	33.26	6.5	0
October	4.03	30.05	30.35	0
November	-0.35	24.21	64.05	3.83
December	-6.95	17.01	43.98	11.83
January	-7.18	16.2	29.63	13
February	-11.38	15.66	58.11	17.5
March	-6.5	18.65	43.03	11

Abdelhamid and et al., (2020) were investigated the relationship between UCS,  $V_p$ , spatial attenuation, and porosity of the five types of Chinese limestone in the end of every 10 F-T cycles. Results indicated that at the end of 40th cycles, there was a high correlation between loss ratios of unconfined compressive strength and spatial attenuation loss with an R2 of 0.8584. Furthermore, there was also a strong relationship between loss ratios of unconfined compressive strength and compressional wave velocity decrease after the end of 20th and 50th cycles with an R2 of 0.9089 and 0.9025, respectively. Gonzalez and et al., (2019) were studied the combined effect of P-wave velocity, saturated density, and porosity on UCS for saturated cylindrical samples of limestone. The results of the multiple exponential models showed that UCS depends directly on  $V_p$  and inversely on  $n$ . Jamshidi and et al., (2018) have investigated the effects of porosity and density on the correlation between uniaxial compressive strength and P-wave velocity for eighteen limestone samples. The results of the investigation indicated that  $\rho$  and  $n$  were effective on the correlation between UCS and  $V_p$  with high determination coefficients. Matsuoka (1990) conducted a laboratory study on the freezing behavior and frost shattering of rocks. The results showed that the main reason for frost shattering was the relative magnitude between the two positive strains. The effect of water saturation on highly porous welded tuff due to F-T cycles was investigated by Chen et al., (2004). They found that cracks created by F-T have a radial pattern when the initial degree of saturation is more than 90%.

Since karst area under study is affected by glacial processes. Therefore, the study will investigate the effect F-T cycles on creating microcrack and microfractures in the samples as the initial factor for accelerating dissolution. The previous studies don't use the factors such as  $n_e$  and  $W_a$  in the determination of decay constant values of limestones subjecting to freezing-thawing cycles. Also, a few studies have calculated the softening and freezing coefficients, and investigate relationships between these coefficients with the loss rate of the strength of limestones. Regarding the difficulty and lengthiness of the F-T test, the present study was conducted to determine the softening and freezing coefficients of four limestone samples and investigate the relationship between these factors with the lithological and physical properties of limestone. The lithology and microfacies properties are analyzed through thin section studies. In addition to investigating the critical mechanical and physical properties of the samples, their behaviors under F-T conditions or in contact with water were studied as well.

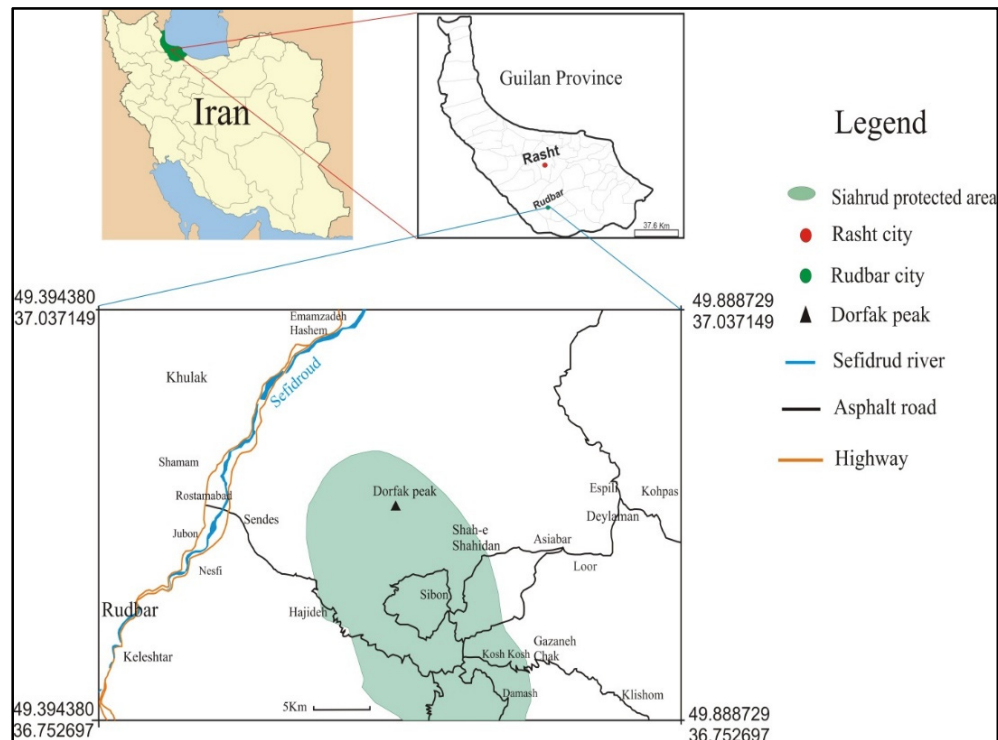
### **Geology and climate of the study area**

The study area is located in northeast Rudbar city; Guilan province, north of Iran (Fig. 1). The dominant climate in the study area is Csa and Bsk according to the Köppen climatic classification system. The surface area of the studied region is 916.30 km<sup>2</sup>. The average annual precipitation and mean temperature were about 748 mm and 1°C, respectively, in the region. The type of predominant weathering was perched in the moderate decomposition with frost action class according to Fookes et al. (1971) graph and meteorological data of the study area (Fig. 2). The study area is located within the structural zone of central and western Alborz. A wide variety of stratigraphic units, ranging in age from Permian to Quaternary, can be observed in the area (Fig. 3). According to field surveys and frequency of karst features in the region, four lithological units were investigated in this study: K11, K12, Km2, and Jk1. The K11 lithological unit contains medium-bedded to massive Orbitolina-bearing limestone with Cretaceous age. Other Cretaceous rocks are characterized by limestone, marl, sandstone, and sandy limestone, thin- to-medium-bedded (Km2 unit), and thin and well-bedded limestone and argillaceous limestone, locally with intercalation of andesitic lava (K12 unit). The Jk1 Jurassic lithological unit is comprised of fossiliferous limestone, locally chert-bearing thick-bedded to massive layers. The Dorfak peak has a pop-up structure that has been created by the enclosure between two Dorfak thrust faults with a slope toward the south and the Deylaman thrust fault

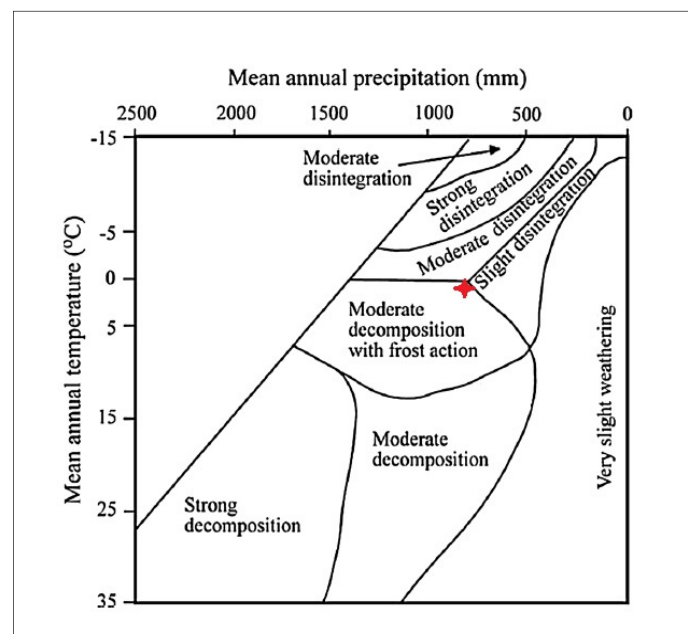
with a slope toward the north.

## Material and method

Four rock samples, taken from the lithological units of K11, K12, Km2, and Jk1, located in the northeast of Rudbar city, were used in this study. These lithological units were chosen because the most karst features have been unfolded in them.



**Figure1.** location map of the study area



**Figure2.** Determination of predominant weathering type of study area (after Fookes et al. 1971)

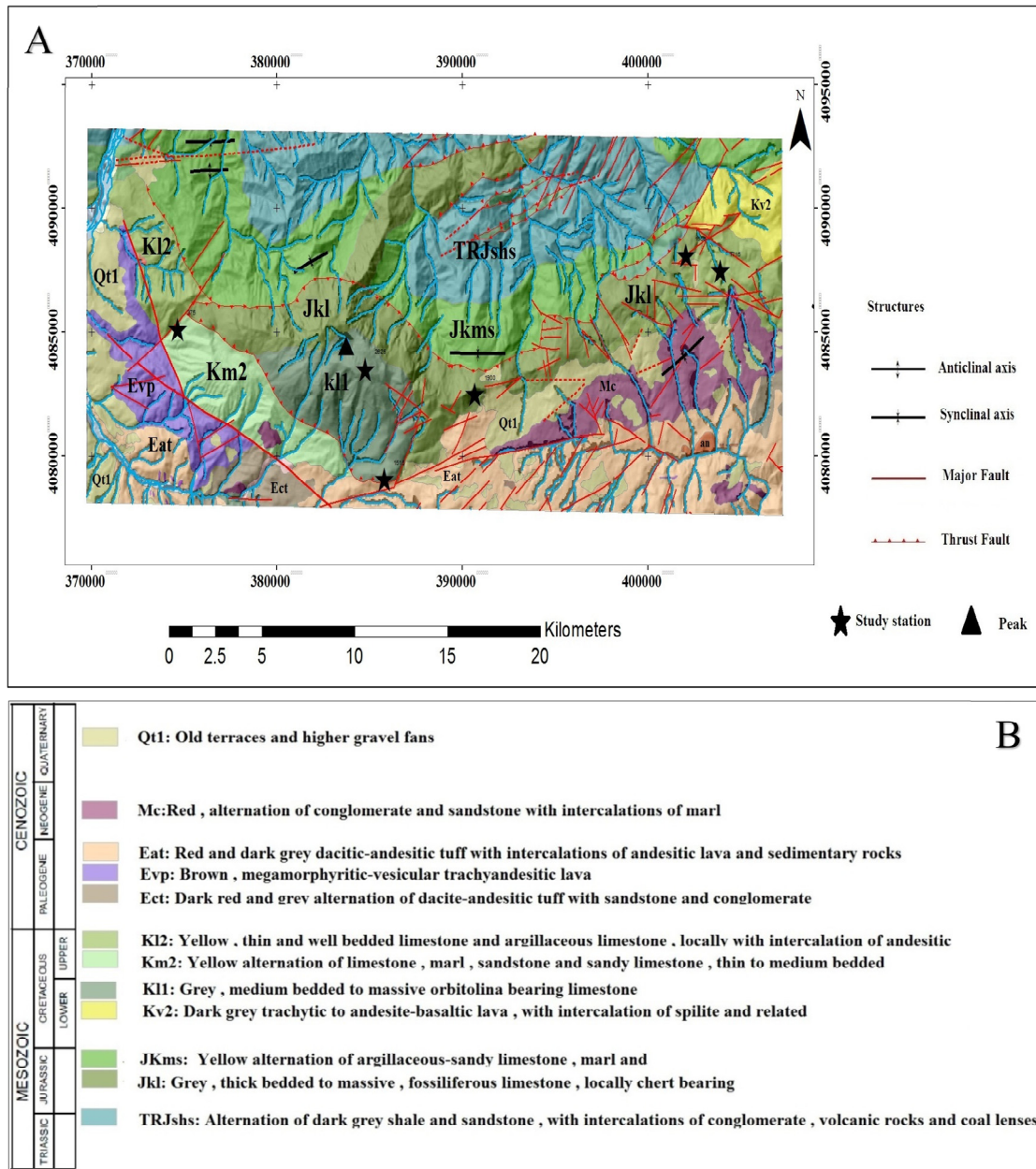


Figure3. Geology map of the study area (A: map, B: legend)

These samples have different physical and mechanical properties, which allows investigating the effect of these properties on rocks frost weathering as a favorable factor for dissolution development. Cylindrical samples (54-55 mm in diameter) were prepared in the laboratory using an apparatus with a diamond bit. The samples were cored perpendicular to bedding plans. All laboratory analytical methods are performed according to the current ISRM and ASTM standards. The methodology of this study is illustrated in Fig. 4. Numbers and dimensions of the samples used for chemical, physical and mechanical laboratory tests are presented in Table 2. The two series thin section was prepared before and after F-T cycles.

*Test Procedures*

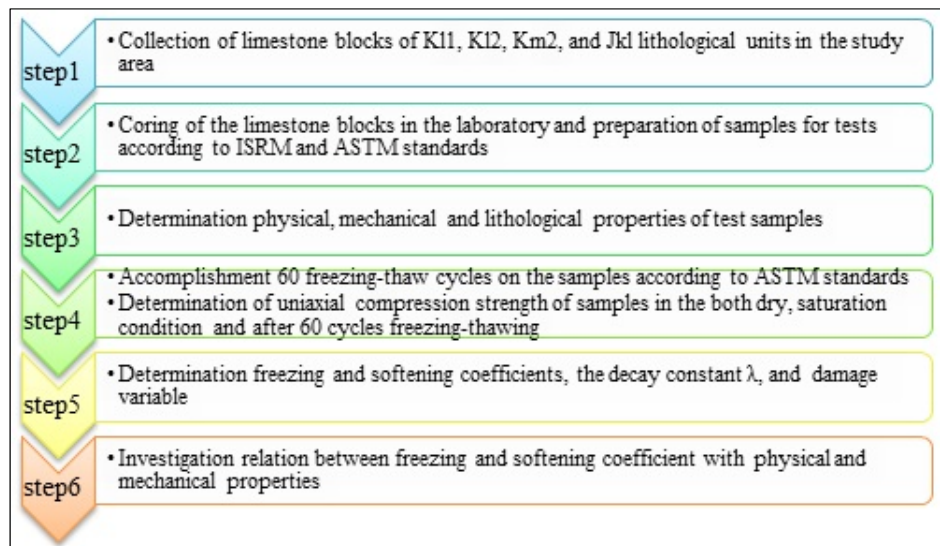
The CaCO<sub>3</sub> content of the studied samples was determined through the back titration process.



In the method, each sample is floured in the mill system and then the powder is screened using sieve #200. About 3 gr of each sample was used for determining the calcite content in three titration tests (Fig. 5).

**Table2.** The sample number and Standards

Test type	Dimention		Sample number	Standard
	Diameter(mm)	Length(mm)		
Freezing-Thawing	55.2-55.76	140.26-150.145	20	ASTM D-5312
UCS <sub>ft</sub>	55.2-55.76	140.26-150.145	20	ISRM
UCS <sub>sat</sub>	54.23-55.75	138.88-164.92	20	ISRM
UCS <sub>dry</sub>	55.54-55.82	138.96-151.91	20	ISRM
BTS	54.22-55.84	27.18-38.45	40	ASTM D-3967
P-wave velocity	55.2-55.76	140.26-150.145	20	ASTM D2845–D2895
Physical propertise	55.54-55.82	138.96-151.91	40	ISRM(1981)
Point load test	Irregular lump		30	ASTM D-5731
Back titration process	Powder (passing of sieve 200#)		12	ASTM D-4739



**Figure4.** Methodology of the study



**Figure5.** The back titration process

In the freezing-thawing (F-T) test, samples were saturated in a 0.5% isopropyl alcohol/water solution, according to ASTM (2004) standard, and stand for a minimum of 12 h. The freezing process was performed using the industrial freezer at -18c for a minimum of 12 h, and the thawing process in the free air at 32c for a minimum of 8 h. F-T cycles were performed on 20 samples of four lithological units in 60 periods (Fig. 6). Determination of 60 cycles was according to the average of frost days in the five consecutive years.

The  $n_e$  (effective porosity) of samples was determined using the vacuum pump under saturation conditions at 48 h. The  $\gamma_{dry}$ ,  $\gamma_{sat}$ ,  $w_a$ , and  $n_e$  were measured following the method introduced by the International Society Rock Mechanics (ISRM) (1981).  $V_p$  was measured using the ASTM standard method (1996). This method measures the transit time of an elastic pulse through the rock sample of a certain sending wave path length. The physical parameter of the sample was measured on the fresh sample and after every 15 F-T cycles.



**Figure 6.** The image of samples before and after 60 freezing-thawing cycles

UCS test was carried out on cylindrical samples having a diameter of 54-55.84 mm and a length-to-diameter ratio of 2.5-3 using a strain gauge to determine the axial strain according (ISRM) in the three conditions dry, saturation, and after 60 F-T cycles. A constant loading rate of 0.5-1 Mpa/s was exerted on all samples. The E was determined for each sample in the three conditions. Also, the Brazilian tensile strength (BTS) test was carried through the ASTM method with a Brazilian apparatus (two steel loading jaws). The tests were conducted on core samples with 54-55.8 mm diameter and height to diameter ratio of 0.5-0.75. The tensile load on the specimen was applied continuously at a constant loading rate (0.5-1 MPa) until failure occurred.

The  $I_{s50}$  was used for the rock sample K12 according to ASTM (2001b). Before the test, the sample was crumbled during 60 F-T cycles. A total of 30 irregular lump tests were performed on specimens with a unit D/W ratio of 1/3 (Fig. 7). Then, uniaxial compressive strength (UCS) was calculated through Eq. (1).

$$\sigma_c = (14 + 0.175D)I_{s50} \quad (1)$$

Where  $I_{s50}$  is the corrected point load strength index and D is a space between two load cones.

### *Decay function model*

The decay function model proposed by Multuturk et al., (2004) is used to evaluate the long-term durability of samples subjected to the F-T cycles. In this model, the disintegration rate of rock is expressed using the decay constant  $\lambda$  parameter. The integrity loss rate through the weathering effect is comparable to the rock integrity at the beginning of each F-T cycle. The decay function model expressed in the exponential equation is as follows:

$$I_N = I_0 e^{-\lambda N} \quad (2)$$

where  $I_0$  and  $I_N$  are the original integrity and the integrity after N cycles of F-T periods of rock, respectively. The decay factor ( $e^{-\lambda N}$ ) expresses the section of the remaining integrity after N cycles of F-T periods. Also, the mean relative integrity loss by the action of any single period is indicated by the decay constant  $\lambda$ , which was obtained by simple exponential regression analysis from an evolution curve of mechanical and physical properties.

## **Results**

### *Origin of rock samples and petrology*


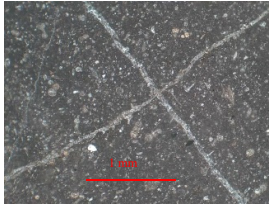
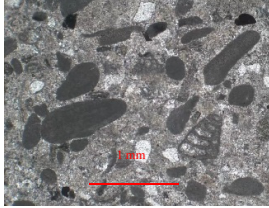

Lithological studies (Table3) were performed using thin sections of the rock samples (K11, K12, Km2, and Jkl Lithological units).



**Figure7.** The some samples of K12 for point load test



**Table 3.** lithological properties of rock samples

Sample name	Ages	Folk system	Mineral composition	Texture	Grain size & Grain boundaries	Pore system	Tin-section
K11	Lower Cretaceous	Biopelsparite	Calcite	Grainstone	Fine Calcarenite to Coarse Calcarenite Sparite filled	Inter particle Moldic	
K12	Upper Cretaceous	Biomicrite	Calcite	Packstone	Very Fine Calcarnite to Fine Calcarnite Micrite filled	Inter particle Fracture	
Km2	Upper Cretaceous	Biosparite	Calcite & Quartz	Grainstone	Fine Calcarenite to Coarse Calcarenite Sparite filled	Inter particle Moldic	
Jkl	Jurassic	Biomicrite	Calcite	Packstone	Fine Calcarenite to Coarse Calcarenite Sparite and Micrite filled	Inter particle Moldic Fracture	

These rocks are grainstone and packstone types according to the Dunham classification (1962). Also, based on Folk classification, they are biopelsparite, biosparite, and biomicrite types. These rocks consisted of skeletal and non-skeletal carbonate grains such as peloid, calcite, and fossil fragments in a micrite and sparite matrix. The skeletal grains are mainly foraminifers and Bivalvia filled with sparite and microcracks, which were also filled with sparite (Table3). The grain fabric and profusion of sparite in the thin section matrix indicate an increase in the turbulence in the sedimentary environment. Moreover, the profusion of micrite in the specimen suggests that they were sedimented in a low-energy environment distal to sources of bioclasts. The fractures filled by sparite and stylolite can be observed in the four types of rock.

### *Physical properties*

Studying the physical properties of rocks is necessary for engineering geology projects. The minerals and microstructures of intact rocks affect the physical properties (Khanlari et al. 2014). Also, the physical properties of intact rocks are highly dependent on the type of rock, texture, percentage, and fabric of minerals forming the rocks (Shalabi et al., 2007). These properties are obtained from four types of cylindrical rock. Average, Standard deviation and variation values for the parameters are shown in Table 4.

The unit Jkl has the maximum dry unit weight, which ranges between 26.22 and 27.02 KN/m<sup>3</sup>

with an average of 26.61. The minimum dry unit weight can be observed in the unit K12, ranging between 25.42 and 25.69 KN/m<sup>3</sup> with an average of 25.50. Also, the same trend can be seen in the saturated unit weights. The maximum water absorption is for unit K12, which is about 1.51%. The maximum effective porosity is for unit K12, varying between 3.28 and 4.27 % with an average of 3.95%. The maximum P-wave velocity is for unit K11, which occurs at the minimum effective porosity. According to the rock classification system suggested by Anon (1979), the samples are classified as rocks with very high dry unit weight and very low to low porosity. The calcite percentages, as the mean value on the basis back titration test for each sample, are presented in Table 4.

### *Mechanical properties*

In this study, the mechanical properties of four limestone types are investigated through performing the uniaxial compressive test (dry, saturation, and after 60 F-T cycles), Brazilian tensile strength test (dry state), and point load test (on sample K12 after 60 F-T cycles). The average values and standard deviation for each test are reported in Table 5. The test samples are located in the moderate strength class, according to Attewell and Farmer's (1976) classification. The saturated compressive strength of the three samples (K11, K12, and Jk1) is increased compared to their dry compressive strength, but sample K12 indicates the inverse condition. The UCS of samples (K11, K12, and Jk1) is decreased after 60 F-T cycles. The point load test shows that sample K12 after 60 F-T cycles fall in the very low strength class corresponding to Bieniawski (1975) and Broch & Franklin's (1972) classifications. The tensile strength of the two samples (K12 and K11) is higher than the other samples.

**Table 4.** physical and chemical properties of rock samples

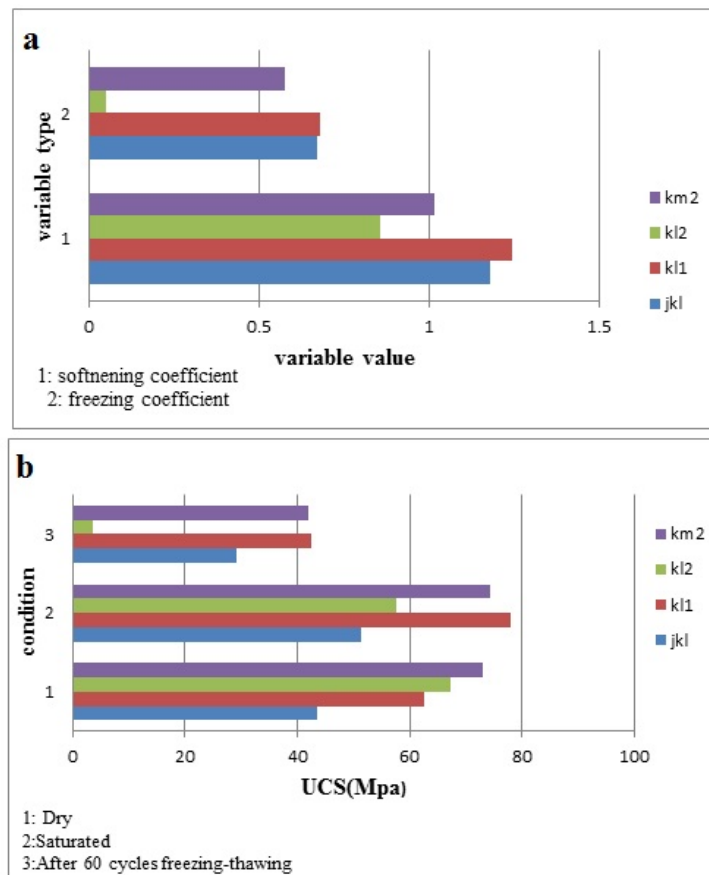
Sample		K11	K12	Km2	Jk1
<b>Calcite %</b>		91.66	89.91	89.5	89.33
	mean	26.60	25.50	26.45	26.61
	Std.	0.2095	0.0850	0.4473	0.2148
<b>γ<sub>dry</sub></b>	Var.	0.04391	0.0072	0.20	0.0461
	mean	26.64	26.23	26.48	26.66
	Std.	0.2112	0.4459	0.4395	0.1835
<b>γ<sub>sat</sub></b>	Var.	0.0446	0.1988	0.1932	0.0337
	mean	0.385	3.955	0.3645	0.51
	Std.	0.0746	0.3259	0.1451	0.5277
<b>n<sub>e</sub> (%)</b>	Var.	0.0055	0.106	0.0210	0.2784
	mean	8982.10	7166.75	8330.42	8651.18
	Std.	496.89	137.32	214.49	218.60
<b>P-wave velocity (m/sec)</b>	Var.	246904.10	18856.81	46008.82	47789.79
	mean	0.14	1.51	0.13	0.19
	Std.	0.0275	0.1293	0.055	0.1994
<b>Wa</b>	Var.	0.00075	0.0167	0.0031	0.0397

**Table 5.** Mechanical properties of rock samples

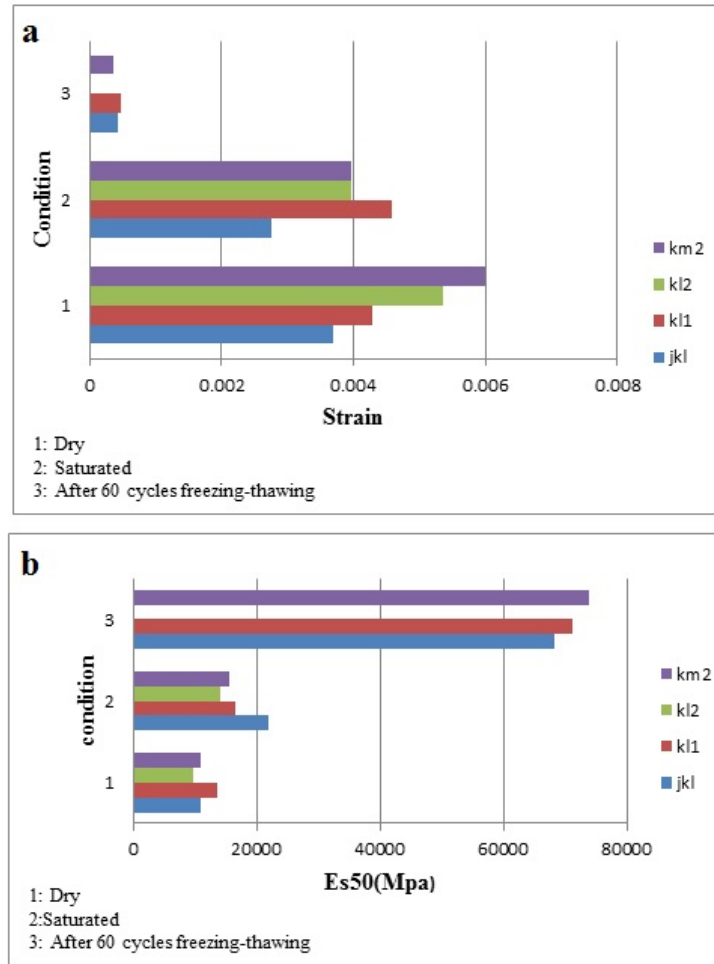
sample	UCS <sub>dry</sub> (Mpa)	Std	UCS <sub>sat</sub> (Mpa)	Std	UCS <sub>f-t</sub> (Mpa)	Std	I <sub>s50</sub> (Mpa)	Std	BTS <sub>dry</sub> (Mpa)	Std
K11	62.60	26.08	77.88	22.14	42.58	18.15			8.65	3.64
K12	67.16	19.97	57.66	29.27	3.43		0.183	0.086	10.83	4.40
Km2	72.99	21.88	74.33	13.41	42.06	17.85			10.42	2.10
Jk1	43.40	10.29	51.21	18.22	29.19	1.29			8.22	2.09

*Calculation of softening and freezing coefficients*

An important durability index of rocks for F-T cycles is the softening and freezing coefficients. The ability of the rock to resist for negative effects of mechanical and chemical agents is expressed as durability (Bednarik et al., 2014). The negative effects on the rock emerge as in the form of loss of strength, disintegration, color changes, etc. (Siegesmund et al., 2002). The decrease in the strength of rock samples by water saturation can be expressed by calculating the softening coefficient ( $K_1$ ), which is the ratio of the UCS of the saturated rock sample to UCS of the dry rock sample (Bednarik et al., 2014). The reduction in the UCS of samples subjected to 60 alternating F-T cycles was expressed with the coefficient of freezing ( $K_2$ ), which is calculated as the ratio of the UCS after 60 F-T cycles to the UCS of the dry rock sample (Bednarik et al., 2014). The  $K_1$  and  $K_2$  coefficients were currently below 1.0, confirming a decrease in the UCS caused by either the saturation or F-T processes. However, some rocks showed an increase in the UCS values, which could indicate changes in the structure of the rock through saturation, or the F-T process (Bednarik et al., 2014). The saturated UCS values of the three samples ( $K_{11}$ ,  $K_{m2}$ , and  $J_{k1}$ ) are higher than the dry UCS values, which is due to the heterogeneity of rock (Fig. 8b). The increase in Young's modulus and the decrease in strain in the peak strength confirm these results (Figs. 9a, 9b, and 9c). The  $K_1$  values higher than 1.0 indicates the high strength of these three samples for wetting-drying processes (Fig. 8a). The lower UCS values after 60 F-T cycles than UCS values of dry samples are attributed to microcrack and fracture development in rock cylinders due to the effect of F-T cycles (Fig 10).



**Figure 8.** Diagrams of mechanical properties. a. Relationship between the  $k_1$  and  $k_2$  coefficients, calculated from average UCS values. b. Results for dry UCS, for saturated UCS, and for UCS following freeze-thaw tests, based on average values.



**Figure 9.** Diagrams of mechanical properties. a. Results for strain for three conditions of dry, saturated, and after 60 freezing-thawing cycles, based on average values. b. Results for tangent modules in the 50% ultimate strength for three conditions of dry, saturated, and after 60 freezing-thawing cycles, based on average values.

The UCS of the K12 sample was calculated through the point load test due to serious damages of samples. The clay minerals per-existing in the sample adsorbed water during 60 F-T cycles and led to the fracture development through an increase in swelling pressure within the specimens.

#### *Determination of damage variable*

The P-wave velocity ( $V_p$ ) of rocks is because of their mineral composition, porosity, and clay percentage (Domenico, 1984; Han et al., 1986; Yu et al., 2015). The  $V_p$  was measured several times every 15 days on samples during 60 F-T cycles. In Fig. 12a,  $V_p$  measurement results of samples (K11, Km2, and Jkl) are plotted as a function of the number of F-T cycles. As can be seen, the  $V_p$  of rock samples declined with an increase in the number of F-T cycles, which is due to changes in microstructure and mechanical performance. The damage variable ( $D_n$ ) was determined through Eq. (3), which is based on the macroscopic phenomenological damage mechanics (Oda et al., 1984; Yu et al., 2015).

$$D_n \approx 1 - \left( \frac{V_{pn}}{V_{p0}} \right)^2 \quad (3)$$



Where  $V_{pn}$  is the P-wave velocity of samples after  $n$  (1, 2...) F-T cycles and  $V_{p0}$  is the initial P-wave velocity of samples before F-T cycles. The relationship curve between damage value ( $D_n$ ) and the number of F-T cycles are preened in Fig. 11. The damage variable ( $D_n$ ) of samples was increased by increasing the number of F-T periods. The linear equation of a curve is as follows.

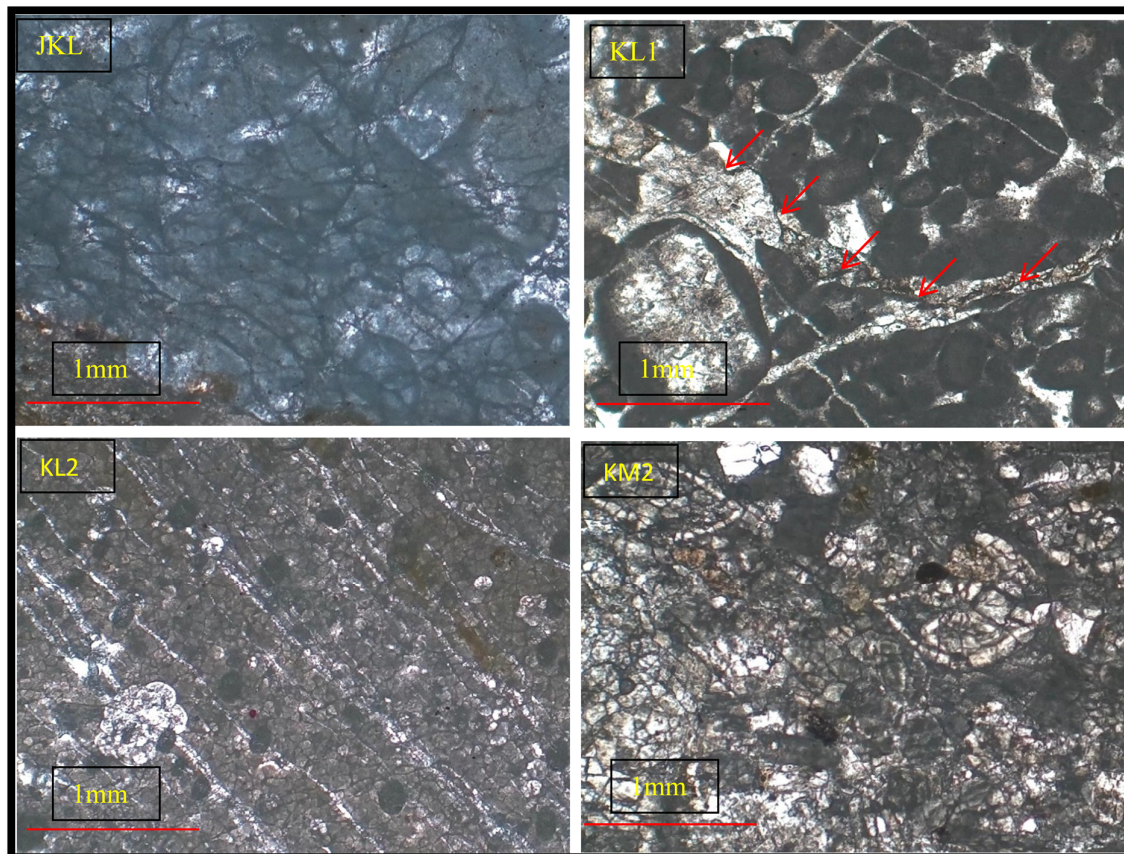
$$D_n = 0.0086N - 0.0138 \quad (4)$$

The values lower than 1.0 of  $D_n$  indicate that the microcracks are created during the F-T cycles. Hence, the damage degree of samples due to the F-T cycles can be estimated based on  $D_n$  values.

#### *Determination of the decay constant value*

The durability of rock samples against the F-T cycles was investigated through the decay function model represented in Eq. (2). The decay constant values ( $\lambda$ ) were calculated for all rock samples (except KL2, because it is highly decayed) through evaluating the  $V_p$ ,  $W_a$ , and  $n\%$  curve during the F-T cycles (Table 6). The evolution of  $V_p$ ,  $W_a$ , and  $n\%$  for 60 cycles of the F-T through determining  $\lambda$  by simple regression analysis is presented in Fig. 12. The best-fit curves were obtained in the excel software based on the determination coefficient ( $R^2$ ). The values of  $\lambda$  and  $R^2$  of different parameters for rock samples are presented in Table 6. The  $R^2$  values obtained from all parameters can be generalized for all rock samples.

The rapid disintegration rate can be distinguished through the high decay constant values (a sudden decrease or increase in the investigated parameters value).



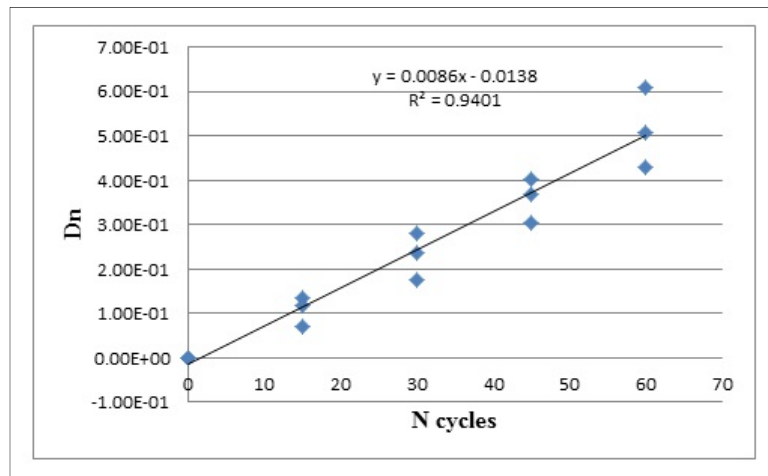
**Figure10.** The microscopic image after 60 cycle's freezing-thawing of the four rock sample (The red flesh showed microfracture)



The decay constant values obtained from different parameters for two samples (K11 and Jk1) have close values; however, such a relationship is not observed in sample Km2 (Table 6).

**Table 6.** The decay constant values ( $\lambda$ ) and the determination coefficient values of rock samples

Sample	$V_p$			$W_a$			n%		
	Equation	$\lambda$	$R^2$	Equation	$\lambda$	$R^2$	Equation	$\lambda$	$R^2$
K11	$y = 9188e^{-0.005x}$	0.005	0.96	$y = 0.1638e^{0.0074x}$	0.0074	0.99	$y = 0.4329e^{0.0076x}$	0.0076	0.99
K12	-	-	-	-	-	-	-	-	-
Km2	$y = 8457e^{-0.006x}$	0.006	0.97	$y = 0.2071e^{0.0136x}$	0.0136	0.96	$y = 0.54e^{0.0139x}$	0.0139	0.96
Jk1	$y = 8966.5e^{-0.008x}$	0.008	0.94	$y = 0.1307e^{0.0075x}$	0.0075	0.97	$y = 0.3415e^{0.0079x}$	0.0079	0.96



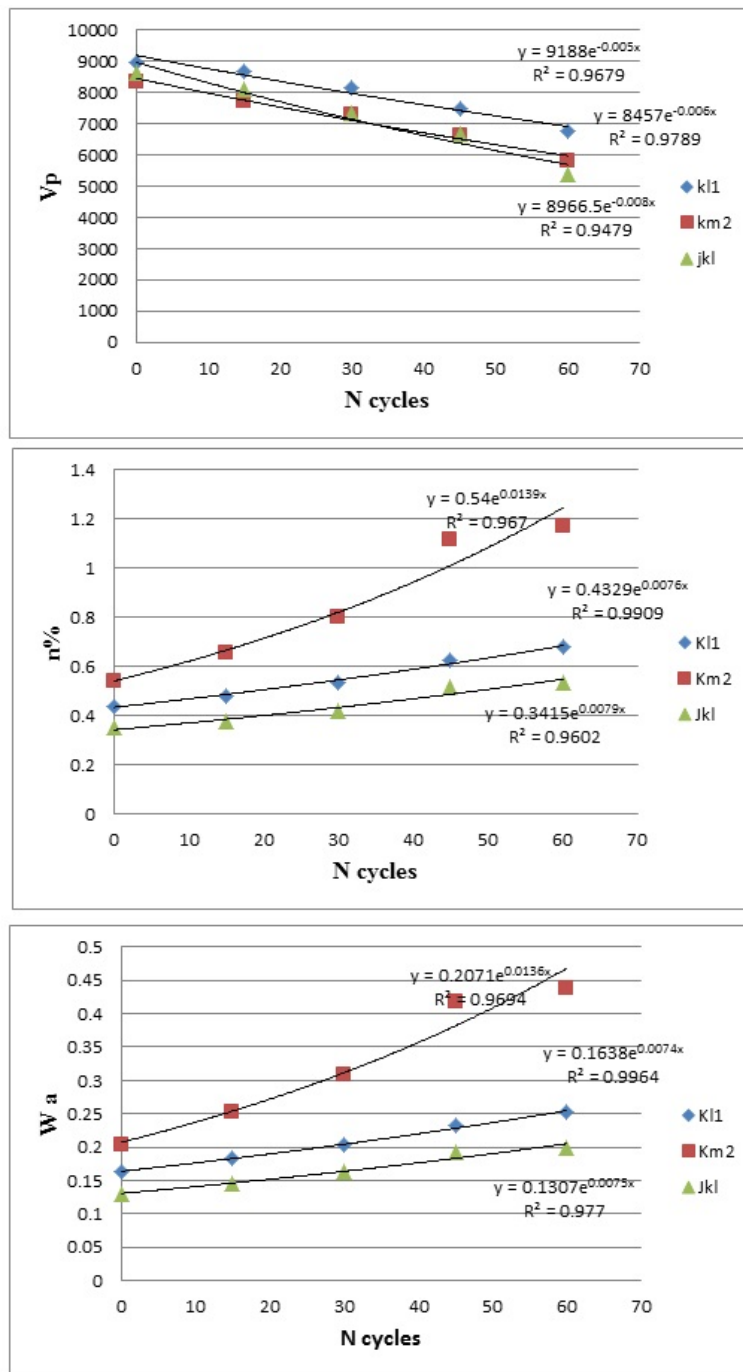
**Figure 11.** Diagram of the  $D_n$  values variation against the number of freezing-thawing cycles

## Discussion

The decadence of rock samples was processed under repeated F-T cycles, which gradually declined their integrity and strength. Most researchers (Matsuoka 1990; Horii et al., 1998; Mutluturk et al., 2004; Chen et al., 2004; Yavuz et al., 2006; Takarli et al., 2008; Bayram, 2012; Bednarik et al., 2014; Ghobadi & Torabi-Kaveh., 2014; Yu et al., 2015; Al-Omari et al., 2015; Eslami et al., 2018) propose the following decadence mechanism for the rocks. The volume shrinkage of mineral grains and the volume expansion of 9% between water stored in the initial micropores and microcracks are two effects for the freezing of rocks. Huge local tensile and compressive stresses were created due to this expansion in the minerals' boundary. These stresses are known collectively as the frost-heave force. The micropores and microcracks were increased due to the frost-heave force acting on the rock. The damage of rocks was accelerated when water flows through the fractured micropores and microcracks after the thawing of the ice. Some of the other external factors affecting the deterioration process are lithological properties, the repetition of F-T cycles (Nicholson et al., 2000), the F-T rate, saturation percent with water (Chen et al., 2004; Stück et al., 2013; De Kock et al., 2017), the temperature variation during F-T cycles (Chen et al., 2004), the interlocking of the crystals and also their porosity (Ruedrich et al., 2011). Thermal dilatation is another decay process that occurs during F-T cycles due to heating and cooling process in the specific temperature ranges; i.e., -18 to 32°C in the ASTM (2004) (Luque et al. 2011; Sun et al. 2017; Siegesmund et al., 2018; Hashemi et al., 2018). Limestone, like the studied rock samples in this study, was highly sensitive to temperature variations. The directional dilatation due to such variations created stress within

the fabric of the rock, which progressively causes the microcracks. This process is accelerated especially in the presence of the water, leading to the decay of the rocks (Andriani & Germinario 2014; Hashemi et al., 2018). In other words, the durability of rocks against F-T cycles also depends on their strength versus thermal-induced stresses.

Therefore, the influence of temperature changes of F-T cycles on rock durability should be investigated in future studies. As the observable situation in Fig. 10, a network of cracks was developed in the three samples (Jkl, kl2, km2).



**Figure12.** Diagrams of physical properties. a. P-wave velocity against the number of freezing-thawing cycles. b. porosity percent against the number of freezing-thawing cycles. c. water absorption against the number of freezing-thawing cycles.

The other cracks were developed in direction fractures filled with sparite in the k11 sample. With attention to the low porosity and the low water absorption of the three samples (K11, Jk1, and Km2), the thermal- induced stresses were the reason for creating cracks in them. In the next cycles, expansion of water due to freezing was the main reason to formation microcracks. But hydric expansion and expansion due to freezing of water in the voids was the reason for creating microcracks in the K12 samples.

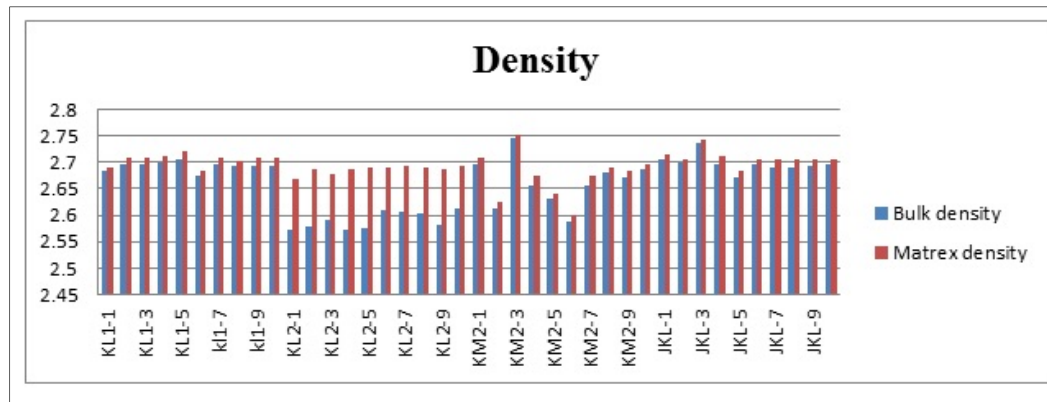
The obtained freezing and softening coefficient values of rock samples indicated that K12 samples have lower durability versus F-T cycles (Fig. 8a) than the other rock samples (K11, Km2, and Jk1). These rock samples have high porosity (Table 3) and the lowest strength under two conditions of saturated and after 60 F-T cycles (Fig. 8b) than the other rock samples. Therefore, the physico-mechanical properties of the K12 sample were made it more susceptible to weathering. Jk1, K11, and Km2 rock samples were more durable in the F-T cycles due to their higher strength and very low porosity in comparison with sample K12. The low porosity, the low water absorption, and heterogeneity of the three samples (K11, Km2, and Jk1) were the main reasons for the higher saturation UCS of these samples.

Three types of crack during the investigation about the cracking mechanisms of rocks were determined in previous studies: 1) wing cracks, 2) quasi-coplanar secondary cracks, and 3) oblique secondary cracks. The wing cracks initiate from the tips of pre-existing flaws based on the tensile formation mechanisms, whereas oblique secondary crack and quasi-coplanar secondary crack initiate due to shear formation mechanisms (Zhou et al., 2014; Hashemi et al., 2018). The stresses induced within rock fabric due to F-T or thermal changes were tensile type (Ruedrich et al., 2011; Hashemi et al., 2018). Therefore, the cracks created and developed within rock fabric due to F-T cycles were mainly wing crack types with tensile formation mechanisms. The competent agents the formation of wing cracks were included the stress intensity, the rock strength, the amount of pre-existing cracks, the temperature variations during the test (Zhou et al., 2018a; Zhang et al., 2018; Hashemi et al., 2018), pore space, and mineralogy composition of rocks. The sedimentary rocks containing clay minerals can generate additional tensile stresses within the rock, due to hydration and swelling of clay minerals during F-T cycles (Bortz & Wonneberger., 1997). Pore space is a characteristic of rock's internal structure that can vary by F-T periods. The durability and the extent of any damage can affect by properties of pore spaces, such as their shapes, their interconnection degree, and their size distributions (Bednarik et al., 2014). The "positive" size pore distribution can create a low water absorption in the rock, which is an essential factor for the rock durability increase against F-T cycles due to the prevented capillary action of water (Bednarik et al., 2014). However, the rocks having pore spaces with specific particular dimensions can resist F-T cycles due to the existence of enough space for lowering the ice expansion pressure.

Therefore, the low freezing coefficient of the K12 sample can also be attributed to the mineralogy of specimen (presence of clay mineral), porosity, and pre-existing cracks in the creation and development of wing cracks. In the other samples, the main agents for the formation and development of wing cracks were the porosity, pre-existing cracks filled with spare calcite, Stylolite and the different rate of expansion and shrinkage between spare calcite and micrite. Still, the higher freezing coefficient of these samples indicates their higher strength in comparison with sample K12. Also, the low water absorption of the three samples (K11, Km2, and Jk1) was indicated on the "positive" size pore distribution. But the expansion and shrinkage due to the thermal change was the main reason for creating tensile and compression stress in these samples in initial cycles of F-T. Then, the expansion of water due to freezing in the new voids was created tensile stress. Therefore the network of cracks with different mechanisms can observe in the three samples. The increase of water absorption and porosity and the decrease of  $V_p$  was the reason for the idea.

The highly compacted carbonate rocks nearly follow the trend of the plutonic rocks

(Siegesmund & Dürrast., 2014). The highest P-wave velocities are therefore more or less parallel to the fracture planes and the lowest perpendicular (Siegesmund & Dürrast, 2014). The high values than the Normal range of  $V_p$  in the initial samples were attributed to low porosity, high compaction, and more or less parallel discontinuity to the axis of samples. The calculation of the bulk density ( $\rho_{Bulk}$ ) and the matrix density ( $\rho_{matrex}$ ) of samples has related to the low porosity (Fig.13).



**Figure13.** The values of matrix and bulk density of samples

## Conclusion

In this paper, the durability of 4 limestone samples was investigated against F-T cycles. The results showed that the physical, mechanical, and petrographic properties of fresh samples have shown that were highly heterogenic. Km2 samples had higher strength and lower effective porosity in dry conditions. The high standard deviation values of UCS have indicated heterogeneity of samples. The  $K_1$  values higher than 1 of Km2, K11, and Jkl are showed higher strength in the saturation condition but the K12 was inverse. The decrease of strain and increase of tangent Young module has proven that the samples were brittle after saturation and 60 F-T periods. By attention to  $D_n$  values, during 60 cycles of F-T has created microfractures which are observable in Fig.10. Although  $V_p$  is an effective tool for calculation  $\lambda$  but,  $n_e$  and  $W_a$  are appropriate to calculate decay constant values. The K12 sample has a rapid disintegration rate but because of the destruction of the sample in the initial cycles F-T, don't calculate the decay constant value. The other samples, Jkl, Km2, and K11 are located next degree in terms of the decay constant. During F-T cycles, will exist the formation possible of tensile and compression stress. Therefore, different types of crack will be formed in rock samples.

## Acknowledgment

The study was performed in the rock mechanic laboratory of Bu-Ali Sina University and was supported by this university.

## References

- Abdelhamid, M.M.A., Li, D., Ren, G., 2020. Predicting Unconfined Compressive Strength Decrease of Carbonate Building Materials against Frost Attack Using Nondestructive Physical Tests. *Sustainability*, 12:1379, 1-18.
- Andriani, G.F., Walsh, N., 2007. Rocky coast geomorphology and erosional processes: a case study along the Murgia coastline South of Bari, Apulia—SE Italy. *Geomorphology*, 87: 224-238.
- Andriani, G.F., Germinario, L., 2014. Thermal decay of carbonate dimension stones: fabric, physical

- and mechanical changes. *Environmental Earth Science*, 72: 2523-2539.
- Attewell, P.B., Farmer, I.W., 1976. *Principles of engineering geology*, Chapman and Hall, London. 1075pp.
- Anon, O.H., 1979. Classification of rocks and soils for engineering geological mapping. Part 1: rock and soil materials. *Bulletin of Engineering Geology and the Environment*, 19: 355-371.
- ASTM., 1995. Standard test method for unconfined compressive strength of intact rock core specimens. ASTM standards on disc 04.08, Designation, D2938.
- ASTM., 1996. Standard test method for laboratory determination of pulse velocities and ultrasonic elastic constants of rock. Designation, D2845-D2895.
- ASTM., 2001b. Standard method for determination of the point load strength index of rock. ASTM standards on disc 04.08, Designation, D5731.
- ASTM., 2004. Standard Test Method for Evaluation of Durability of Rock for Erosion Control Under Freezing and Thawing Conditions. Designation, D5312 - 04.
- ASTM., 2011. Standard Test Method for Base Number Determination by Potentiometric Hydrochloric Acid Titration, ASTM international, West Conshohocken, PA, 2003, Standard D4739.
- Al-Omari, A., Beck, K., Brunetaud, X., Török, Á., Al-Mukhtar, M., 2015. Critical degree of saturation: A control factor of freeze-thaw damage of porous limestones at Castle of Chambord, France. *Engineering Geology*, 185: 71-80.
- Bayram, F., 2012. Predicting mechanical strength loss of natural stones after freeze-thaw in cold regions. *Cold Regions Science and Technology*, 84: 98-102.
- Bednarik, M., Moshhammer, B., Heinrich, M., Holzer, R., Laho, M., Rabeder, J., Uhlir, C.H., Unterwurzacher, M., 2014. Engineering geological properties of Leitha Limestone from historical quarries in Burgenland and Styria, Austria. *Engineering Geology*, 176: 66-78.
- Beier, N.A., Segó, D.C., 2009. Cyclic freeze-thaw to enhance the stability of coal tailings. *Cold Regions Science and Technology*, 55: 278-285.
- Bellanger, M., Homand, F., Remy, J.M., 1993. Water behaviour in limestones as a function of pores structure: application to frost resistance of some Lorraine limestones, *Engineering Geology*, 36: 99-108.
- Bieniawski, Z.T., 1975. The point load test in geotechnical practice, *Engineering Geology*, 9: 1-11.
- Bortz, S.A., Wonneberger, B., 1997. Laboratory evaluation of building stone weathering. In: Labuz, J.S., (Ed.), *Degradation of Natural Building Stone*. Geotechnical Special Publications, 72: 85-104.
- Broch, E., Franklin, J.A., 1972. The point-load strength test. *International Journal Rock Mechanics and Mining Sciences & Geomechanics Abstract*, 9: 669-698.
- Chen, C.H., Yeung, M.R., Mori, N., 2004. Effect of water saturation on deterioration of welded tuff due to freeze-thaw action. *Cold Regions Sciences Technology*, 38: 127-136.
- De Kock, T., Turmel, A., Fronteau, G., Cnudde, V., 2017. Rock fabric heterogeneity and its influence on the petrophysical properties of a building limestone: Lede stone (Belgium) as an example. *Engineering Geology*, 216: 31-41.
- Domenico, S.N., 1984. Rock lithology and porosity determination from shear and compressional wave velocity. *Geophysics*, 49: 1188-1195.
- Eslami, J., Walbert, C.H., Beaucour, A., Bourges, A., Noumowe, A., 2018. Influence of physical and mechanical properties on the durability of limestone subjected to freeze-thaw cycles. *Construction and Building Materials*, 162: 420-429.
- Everett, D.H., 1961. The thermodynamics of frost damage to porous solids, *Transactions of the Faraday Society*, 57: 1541-1551.
- Fereidooni, D., Khajevand, R., 2017. Correlations Between Slake-Durability Index and Engineering Properties of Some Travertine Samples Under Wetting Drying Cycles. *Journal of Geotechnical Engineering*, 36: 1071-1089.
- Fookes, P.G., Dearman, W.R., Franklin, J.A., 1971, Some engineering aspects of rock weathering with field examples from Dartmoor and elsewhere. *Quarterly Journal of Engineering Geology and Hydrogeology*, 5: 139-185.
- Ghobadi, M.H., Torabi-Kaveh, M., 2014. Assessing the potential for deterioration of limestones forming Taq-e Bostan monuments under freeze-thaw weathering and karst development. *Environmental*



- Earth Sciences, 72: 5035-5047.
- González, J., Saldaña, M., Arzúa, J., 2019. Analytical Model for Predicting the UCS from P-Wave Velocity, Density, and Porosity on Saturated Limestone. *Applied Sciences*, 9(23): 52-65.
- Han, D.H., Nur, A., Morgan, D., 1986. Effects of porosity and clay content on wave velocities in sandstones. *Geophysics*, 51: 2093-2107.
- Hashemi, M., Bashiri Goudarzi, M., Jamshidi, A., 2018. Experimental investigation on the performance of Schmidt hammer test in durability assessment of carbonate building stones against freeze-thaw weathering. *Environmental Earth Sciences*, 77(684):1-15.
- Hassanvand, M., Moradi, S., Fattahi, M., Zargar, G.H., 2018. Estimation of rock uniaxial compressive strength for an Iranian carbonate oil reservoir: Modeling vs. artificial neural network application. *Petroleum Research*, 3: 336-345.
- Hori, M., Morihiro, H., 1998. Micromechanical analysis on deterioration due to freezing and thawing in porous brittle materials. *International Journal of Engineering Science*, 36: 511-522.
- ISRM., 1981. ISRM suggested methods. In: Brown, E.T., (Ed.), *Rock characterization, testing and monitoring*. Pergamon Press, London, 211pp.
- Jamshidi, A., Zamanian, H., Zarei Sahamieh, R., 2018. The effect of density and porosity on the correlation between uniaxial compressive strength and P-wave velocity. *Rock mechanics and Rock engineering*, 51(4): 1279-1286.
- Jamshidi, A., Nikudel, M.R., Khamehchiyan, M., 2016. Evaluation of the durability of Gerdoe travertine after freeze-thaw cycles in fresh water and sodium sulfate solution. *Engineering Geology*, 202: 36-43.
- Jamshidi, A., Nikudel, M.R., Khamehchiyan, M., 2015. Estimating the engineering properties of building stones after freeze-thaw using multiple regression analysis. *Iranian Journal of Sciences and Technology, Transaction A: Science*, 39A2: 147-163.
- Jamshidi, A., Nikudel, M.R., Khamehchiyan, M., 2013. Predicting the long-term durability of building stones against freeze-thaw using a decay function model. *Cold Regions Sciences and Technology*, 92: 29-36.
- Khanlari, G.R., Heidari, M., Sepahi-Gero, A. A, Fereidooni, D., 2014. Quantification of strength anisotropy of metamorphic rocks of the Hamedan province, Iran, as determined from cylindrical punch, point load and Brazilian tests. *Engineering Geology*, 169: 80-90.
- Koch, A., Siegesmund, S., 2004. The combined effect of moisture and temperature on the anomalous expansion behaviour of marble. *Environmental Geology*, 46: 350-363.
- Luque, A., Ruiz-Agudo, E., Cultrone, G., Sebastia'n, E., Siegesmund, S., 2011. Direct observation of microcrack development in marble caused by thermal weathering. *Environmental Earth Sciences*, 62: 1375-1386.
- Multuturk, M., Altindag, R., Turk, G., 2004. A decay function model for the integrity loss of rock when subjected to recurrent cycles of freezing-thawing and heating-cooling, *International Journal of Rock Mechanics and Mining Sciences*, 41: 237-244.
- Matsuoka, N., 1990. Mechanisms of rock breakdown by frost action: an experimental approach. *Cold Regions Sciences and Technology*, 17: 253-270.
- Nicholson, H., Dawn, T., Nicholson, F.H., 2000. Physical deterioration of sedimentary rocks subjected to experimental freeze-thaw weathering. *Earth Surface Processes and Landforms*, 25: 1295-1307.
- Oda, M., Suzuki, K., Maeshibu, T., 1984. Elastic compliance for rock-like materials with random cracks. *Soils and Foundations*, 24: 27-40.
- Pápay, Z., 2018. Effect of Thermal and Freeze-thaw Stress on the Mechanical Properties of Porous Limestone. *Periodica Polytechnica Civil Engineering*, 62(2): 423-428.
- Plevová, E., Kozušni'kova, A., Vaculí'kova, L., Simha Martynkova, G., 2010. Thermal behavior of selected Czech marble samples. *Journal of Thermal Analysis and Calorimetry*, 101: 657-664.
- Proskin, S., Sego, D., Alostaz, M., 2010. Freeze-thaw and consolidation tests on Suncor mature fine tailings (MFT). *Cold Regions Sciences and Technology*, 63: 110-120.
- Powers, T.C., Helmuth, R. A., 1953. Theory of volume changes in hardened Portland cement paste during freezing. *Proceedings of the annual meeting - Highway Research Board*, 32: 285- 297.
- Ruedrich, J., Kirchner, D., Siegesmund, S., 2011. Physical weathering of building stones induced by freeze-thaw action: a laboratory longterm study. *Environmental Earth Sciences*, 63: 1573-1586.
- Royer-Carfagni, G. F., 1999. On the thermal degradation of marble. *International Journal of Rock*

- Mechanics and Mining Sciences, 36: 119-126.
- Saad, A., Guedon, S., Martineau, F., 2010. Microstructural weathering of sedimentary rocks by freeze-thaw cycles: experimental study of state and transfer parameters. *Comptes Rendus Geoscience*, 342: 197-203.
- Setzer, M.J., Seter, M., Auberg, R., 1997. Basis of testing the freeze-thaw resistance Surface and internal deterioration. E & FN Spon London, pp. 157-173.
- Shalabi, F. I., Cording, E. J., Al-Hattamleh, O. H., 2007. Estimation of rock engineering properties using hardness tests. *Engineering Geology*, 90: 138-147.
- Siegesmund, S., Ullemeyer, K., Weiss, T., Tschegg, E.K., 2000. Physical weathering of marbles caused by anisotropic thermal expansion. *International Journal of Earth Sciences*, 89: 170-182.
- Siegesmund, S., Weiss, T., Vollbrecht, A., 2002. *Natural Stone, Weathering Phenomena, Conservation Strategies and Case Studies*. Geological Society, London, 205pp.
- Siegesmund, S., Grimm, W.D., Dürrast, H., Ruedrich, J., 2010. Limestones in Germany used as building stones: an overview. In: Smith, B. J., Go´mez-Heras, M., Viles, H. A., Cassar, J., (Ed.), *Limestone in the built environment: present-day challenges for the preservation of the past*. Geological Society, London, pp 37-59.
- Siegesmund, S., Dürrast, H., 2014. Physical and mechanical properties of rocks. In: Siegesmund, S., Snethlage, R., (Ed.), *Stone in architecture*, 5<sup>th</sup> edn. Springer, Berlin, pp 97-225.
- Stück, H., Plagge, R., Siegesmund, S., 2013. Numerical modeling of moisture transport in sandstone: the influence of pore space, fabric and clay content. *Environmental Earth Sciences*, 69(4): 1161-1187.
- Shushakova, V., Fuller, E. R. Jr., Siegesmund, S., 2011. Influence of shape fabric and crystal texture on marble degradation phenomena: simulations. *Environmental Earth Sciences*, 63: 1587-1601.
- Shushakova, V., Fuller, E. R. Jr., Siegesmund, S., 2013. Microcracking in calcite and dolomite marble: microstructural influences and effects on properties. *Environmental Earth Sciences*, 69: 1263-1279.
- Takarli, M., Prince, W., Siddique, R., 2008. Damage in granite under heating/cooling cycles and water freeze-thaw condition. *International Journal Rock Mechanic and Mining Sciences*, 45: 1164-1175.
- Tan, X., Chen, W., Yang, J., Cao, J., 2011. Laboratory investigation on the mechanical properties degradation of granite under freeze-thaw action. *Cold Regions Sciences and Technology*, 68: 130-138.
- Torabi-Kaveh, M., Heidari, M., Mohseni, H., Menendez, B., 2019. Role of petrography in durability of limestone used in construction of Persepolis complex subjected to artificial accelerated ageing tests. *Environmental Earth Sciences*, 78 (297): 1-18.
- Walbert, C. H., Eslami, J., Beaucour, A., Bourges, A., Noumowe, A., 2015. Evolution of the mechanical behaviour of limestone subjected to freeze-thaw cycles. *Environmental Earth Sciences*, 74: 6339-6351.
- Weiss, T., Siegesmund, S., Fuller, E. R. J. r., 2003. Thermal degradation of marble: indications from finite-element modelling. *Build Environmental*, 38: 1251-1260.
- Yagiz, S., 2011. Correlation between slake durability and rock properties for some carbonate Rocks. *Bulletin of Engineering Geology and the Environment*, 70: 377-383.
- Yagiz, S., 2018. The Effect of pH of the Testing Liquid on the Degradability of Carbonate Rocks. *Geotechnical and Geological Engineering*, 36: 2351-2363.
- Yavuz, H., Altindag, R., Sarac, S., Ugur, I., Sengun, N., 2006. Estimating the index properties of deteriorated carbonate rocks due to freeze-thaw and thermal shock weathering. *International Journal of Rock Mechanics and Mining Sciences*, 43: 767-775.
- Yu, J., Chen, X., Li, H., Zhou, J. W., 2015. Effect of Freeze-Thaw Cycles on Mechanical Properties and Permeability of Red Sandstone under Triaxial Compression. *Journal of Mountain Science*, 12: 218-231.
- Zhou, X. P., Cheng, H., Feng, Y. F., 2014. An experimental study of crack coalescence behavior in rock-like materials containing multiple flaws under uniaxial compression. *Rock Mechanics and Rock Engineering*, 47(6): 1961-1986.
- Zhou, X. P., Zhang, J. Z., Wong, L. N. Y., 2018a. Experimental study on the growth, coalescence and wrapping behaviors of 3D cross embedded flaws under uniaxial compression. *Rock Mechanics and Rock Engineering*, 51(5): 1379-1400.
- Zhang, J. Z., Zhou, X. P., Zhu, J.Y., Xian, C., Wang, Y. T., 2018. Quasi-static fracturing in double-

flawed specimens under uniaxial loading: the role of strain rate. *International Journal of Fracture*, 211(1-2): 75-102.

Zeisig, A., Siegesmund, S., Weiss, T., 2002. Thermal expansion and its control on the durability of marbles. In: Siegesmund, S., Weiss, T., Vollbrecht, A., (Ed.), *Natural stone, weathering phenomena, conservation strategies and case studies*, vol 205, Special Publications. Geological Society, London, pp 65-80.



This article is an open-access article distributed under the terms and conditions of the Creative Commons Attribution (CC-BY) license.